The Development of Loops, Trains, and Tails in a Self-Avoiding Polymer Sequence at a Rigid Boundary as a Function of Solvent Composition

Clive A. Croxton

Department of Mathematics, University of Newcastle, N.S.W. 2308, Australia.
Received February 18, 1987

ABSTRACT: The development of loops, trains, and tails in a self-avoiding hard-sphere sequence terminally attached to a rigid boundary is determined as a function of solvent particle diameter, packing fraction, and chain length: the analysis is made on the basis of the convolution integral approximation. It is found that the introduction of a solvent drastically modifies their development in comparison to the zero solvent case, and the results are analyzed in terms of the attritional processes associated with the introduction of the boundary and the replacement of segment by solvent particles.

Introduction

In a previous paper,[1] we reported the configurational properties of self-avoiding hard-sphere polymer sequences of short to intermediate length as a function of solvent composition. These chains were terminally attached to a rigid boundary, and the configurational properties of the sequence were determined on the basis of the iterative convolution (IC) approximation, whilst the chain was immersed in a Percus–Yevick solvent of hard spheres. It is not appropriate to repeat the details of those calculations here, and we restrict ourselves to the reiteration of the principal conclusions of that analysis.

The segment density profile normal to the rigid boundary is defined by

$$\rho(z|N)_{\eta\sigma_s} = \sum_{i=1}^{N} Z(0i|N)_{\eta\sigma_s} \qquad (1)$$

where $Z(0i|N)_{\eta\sigma_s}$ is the spatial segment-boundary probability distribution of the ith segment within the N-mer along the boundary normal z at solvent packing fraction η and solvent diameter σ_s, respectively. The boundary is designated by 0 throughout. In particular, it was found that $\rho(z|N)_{\eta\sigma_s}$, apart from possessing a discontinuity at one segment diameter from the boundary, developed an oscillatory structure whose amplitude depended upon the solvent packing fraction η and whose period was exactly that of the solvent diameter. Moreover, the boundary contact value ($z = 0$) of the segment density profile developed dramatically with solvent packing fraction, although to an extent inversely related to the solvent diameter. This behavior was understood qualitatively in terms of the entropic processes associated with the introduction of a rigid boundary in an otherwise homogeneous polymer/solvent system. If we consider a hard-sphere system having segments and solvent of the same diameter, then clearly the entropy per particle is lower for the sequentially connected segments than for the solvent particles. If now, for the purposes of simplicity, we assume we have a homogeneous mixture of these two types of particles, then the increase in free energy per unit area of the boundary introduced in minimized by the migration of chain segments rather than solvent particles to the boundary. Sequential connectivity of the chain complicates this simplistic description somewhat, although the qualitative attribution to entropic processes at the boundary remains correct. The consequences of this for the development of loops and trains within the terminally attached sequence are considerable since these configurational states depend sensitively upon the form of $\rho(z|N)_{\eta\sigma_s}$ in the immediate vicinity of the boundary. Indeed, in the absence of a solvent, an earlier convolution analysis[2] of the development of loop, train, and tail states for a terminally attached hard-sphere sequence revealed that the chain was essentially expelled from the immediate vicinity of the boundary, and this was attributed to an effective "entropic repulsion" deriving from the geometrical attrition of chain configurations associated with the presence of the rigid boundary. Under these circumstances, more than 95% of the chain existed in the form of tail states, and this was subsequently confirmed by Monte Carlo simulation.[3]

While there have been earlier continuum theoretical analyses of the configurational properties of terminally attached sequences,[4] these have generally neglected the excluded volume feature to a greater or lesser extent. Accordingly, many of the conclusions drawn have only indirect bearing upon the truly self-avoiding system, and it is inappropriate to review them here. Nevertheless, an early continuum study of Roe[4] which took partial account of the self-avoiding feature of terminally attached sequences yielded results in close agreement with both the convolution and Monte Carlo analyses: lattice-based treatments involving either exact enumeration or Monte Carlo estimates of the configurational properties have been reported,[5,6] and whilst these incorporate the self-avoiding feature to some extent, they nevertheless are but caricatures of their continuum counterparts—and indeed, forfeit some of the detailed structural features observed in such systems.[7]

Theory

Here we briefly review the underlying theoretical description of the approach, whilst referring the reader elsewhere for the details of the technique.[1-3]

Firstly, we introduce the spatial intersegmental probability distributions $Z(ij|N)$ between all pairs of segments i,j within the N-mer. Since $Z(ij|N) = Z(ji|N)$, we are involved in the determination of $(N^2 - 3N)/2$ such distributions within the N-mer: adjacent segments are taken to be sequentially linked at fixed separation, so the $Z(i,i\pm1|N)$ are set as δ functions and do not need to be determined. The Z functions are determined on the basis of an integral equation closely related to the Ornstein–Zernike equation familiar from liquid-state theory and require as input only the specification of the interaction matrix of pair potentials between the set of segments constituting the sequence. Thus the technique can readily handle heterogeneous linear sequences, although here we restrict ourselves to the "pearl necklace" model of identical hard-sphere segments.

Two degrees of approximation to the solution of the integral equation have been investigated: the convolution

0024-9297/88/2221-0244$01.50/0

approximation and the iterative convolution approximation. In both cases, the equations are evaluated by fast Fourier transform techniques, and whilst the latter approximation yields results in somewhat better agreement with Monte Carlo data, the calculations are substantially slower.

This proves to be a crucial aspect in the present case as we shall explain below, and accordingly we are necessarily restricted to the noniterative approach in this treatment. Nevertheless, an earlier investigation of loop, train, and tail development for terminally attached sequences in the absence of a solvent[2] yielded results in good agreement with a Monte Carlo analysis of the system, and accordingly we feel confident in adopting the noniterative approach in the present case.

As in the IC analyses, the presence of a rigid planar boundary is modeled by allowing the diameter of the first segment (designated 0) $\sigma_0 \rightarrow \infty$. In fact, the configurational properties of sequences rapidly approach an asymptotic value with increasing σ_0, $\sigma_0 = 64$ appears to be adequate for $N < 25$, and this value is adopted throughout: Monte Carlo investigations appear to vindicate the adequacy of $\sigma_0 = 64$ as a model for a truly planar boundary within the range of chain lengths indicated above.

The boundary–segment–solvent system is regarded as a three-component fluid of hard-sphere particles having diameters σ_0, σ, and σ_s, respectively. The spatial radial distribution functions $g^{(2)}(r_{ij})_{\eta\sigma_s}$ describing the segment–segment and segment–solvent correlations may be readily determined on the basis of the three-component coupled Ornstein–Zernike equations in the Percus–Yevick approximation. Given that we are working with a hard-sphere system, it remains only to specify the composition of the solvent in terms of its particle diameter σ_s and packing fraction η. With a knowledge of these radial distributions, we may readily determine the potential of mean force $\Psi_{\alpha\beta}$ operating between any two species α,β in the ternary system by means of the Boltzmann relation

$$\Psi(r_{\alpha\beta})_{\eta\sigma_s} = -kT \ln (g^{(2)}(r_{\alpha\beta}))_{\eta\sigma_s} \quad (2)$$

These effective interactions may now be used in the interaction matrix required for the evaluation of the Z functions in the convolution approximation. What these effective interactions represent are the modification of the hard-sphere segment–segment and segment–boundary interactions by the presence of a solvent of diameter σ_s and packing fraction η. Certainly it is not strictly correct to regard the chain–solvent system as a homogeneous mixture of disconnected segments and solvent particles for the purposes of determination of the Ψ functions; however, such an approach has proved highly satisfactory in, for example, the prediction of the equation of state of dense entanglements of polymers in terms of the agreement with Monte Carlo estimates.[9]

The $Z(0i|N)_{\eta\sigma_s}$ may be used to form the segment density profile normal to the boundary (eq 1), whilst the various moments of the distributions $Z(ij|N)_{\eta\sigma_s}$ are used to form the mean square end-to-end length, radius of gyration, etc., and may be investigated as a function of solvent composition. This has been reported elsewhere.[1] Our present concern, however, is with the development of loops, trains, and tails at the boundary, and the resolution, and expression of these structures in terms of the Z functions requires further consideration. Although a detailed description has been given elsewhere,[2] it is appropriate to give a brief outline here for the purpose of completeness.

We firstly adopt a binary representation for the description of a polymer configuration whereby 1(0) represents contact (noncontact). For example, [1000011100] represents a 10-segment chain in which segment 1 is terminally attached to the boundary and segments 2–5 constitute a loop, segments 6–8 a train, and segments 9 and 10 a tail. Loops may be readily identified as internal sequences of zeros, trains as internal sequences of ones, and tails as terminal sequences of zeros. Of course, a precise specification of what constitutes "contact" has to be made, but this presents no problem in practice: a normalized spatial distribution $Z(0i|N)_{\eta\sigma_s}$ may be resolved into contact $Z^{(1)}(0i|N)_{\eta\sigma_s}$ and noncontact $Z^{(0)}(0i|N)_{\eta\sigma_s}$ components, where we take the thickness of the region $z \leq \sigma/16$ (=0.0625 for unit diameter segments) to be the contact zone, ζ. In the convolution approximation, the determination of $Z^{[i]}(0i|N)_{\eta\sigma_s}$ within an N-mer presupposes a knowledge of $Z^{[i]}(0i|N-1)_{\eta\sigma_s}$ within the N-1-mer, and accordingly recursively regresses through sequences of decreasing length until a chain of i segments is reached, involving the distribution $Z[^i](0i|i)_{\eta\sigma_s}$. The superscript $[i]$ specifies a given i-bit binary sequence representing a specific set of contact/noncontact configurations for the first i segments in the N-mer. Thus, $Z^{[i]}(0i|N)_{\eta\sigma_s}$ is given as

$$Z^{[i]}(0i|N)_{\eta\sigma_s} = Z^{[i]}(0i|N-1)_{\eta\sigma_s} \int Z(iN|N)_{\eta\sigma_s} H(0N)_{\eta\sigma_s} \, dN \quad (3)$$

where $H(0N)_{\eta\sigma_s} = \exp(-\Psi(0N)_{\eta\sigma_s}/kT)$ and $Z(iN|N)_{\eta\sigma_s}$ represents the spatial distribution of segments i and N within the N-mer unresolved into contact/noncontact configurations. We note that the determinations of $Z^{[i]}(0i|N)_{\eta\sigma_s}$ are accordingly unconditional with respect to the configurations adopted by segments $i+1,\ldots,N$. As we observed above, the convolution[3] recursively regresses to $Z^{[i]}(0i|i)_{\eta\sigma_s}$ which is defined by

$$Z^{[i]}(0i|i)_{\eta\sigma_s} = H(0i)_{\eta\sigma_s} \int Z^{[i-1]}(0,i-1|i)_{\eta\sigma_s} \, \delta(i-1,i) \, d(i-1) \quad (4)$$

$Z^{[i-1]}(0,i-1|i)_{\eta\sigma_s}$ in (4) is formed by convolving the appropriate sequence of contact/noncontact functions.

The probability of contact of the ith segment in the N-mer is then

$$P^{[i-1,1]}|_{N;\eta,\sigma_s} = \int_{(\sigma_0+\sigma_i)/2}^{\zeta+(\sigma_0+\sigma_i)/2} Z^{[i]}(0i|N)_{\eta\sigma_s} \, dr_{0i} \quad (5)$$

where $[i-1,1]$ represents a given i-1-bit binary sequence for the configuration of the first i-1 segments with the ith segment in contact with the plane. Similarly, for noncontact of the ith segment,

$$P^{[i-1,0]}|_{N;\eta,\sigma_s} = 1 - P^{[i-1,1]}|_{N;\eta,\sigma_s} \quad (5a)$$

where $\zeta = 0.0625$ for unit diameter segments.

Finally, the probability of a given configuration adopted by the N-mer is taken to be the product

$$P^{[N]}|_{\eta,\sigma_s} = \prod_{i=2}^{N} P^{[i-1,\xi_i]}|_{N;\eta\sigma_s} \quad (6)$$

where ξ_i is the bit state of segment i, which assumes the statistical independence of loop, train, and tail configurations within the sequence. Since all configurations of the chain are represented on the binary tree, it follows that the probabilities at a given chain length sum to unity; e.g., for a terminally attached 3-mer

$$P^{[100]} + P^{[101]} + P^{[110]} + P^{[111]} = 1 \quad (7)$$

etc., which represents a criterion for the correct normalization of the distributions. A particular configuration $[N]$ of the N-mer will arise with probability $P^{[N]}$ (eq 6) and be characterized by numbers $n_{\text{loops}}[N]$ and $n_{\text{trains}}[N]$ of

loops and trains, respectively. In addition, the configuration $[N]$ will have a length of loops $L_{loops}[N]$ and of trains $L_{trains}[N]$. Appropriately weighting and averaging over all configurations of the N-mer $\langle\cdots\rangle_{[N]}$ yields the expectation quantities

$$\langle n_{loops}\rangle = \langle n_{loops}[N]P^{[N]}\rangle_{[N]}$$
$$\langle L_{loops}\rangle = \langle L_{loops}[N]P^{[N]}\rangle_{[N]} \quad (8)$$

where $L_{loops}[N] \equiv$ length of the loop in the particular contact sequence $[N]$ and $\langle L_{loops}\rangle \equiv$ ensemble average of $L_{loops}[N]$ for chains of length N, with analogous expressions for the number and length of trains. The average loop length within the chain then follows as $\langle L_{loops}\rangle/\langle n_{loops}\rangle$, similarly for trains.

A tail, on the other hand, either does or does not terminate a configuration $[N]$ and accordingly is or is not included in the expectation probability of tail formation:

$$\langle n_{tail}\rangle = \langle P^{[N]}\rangle_{[N]}$$
$$\langle L_{tail}\rangle = \langle L_{tail}[N]P^{[N]}\rangle_{[N]} \quad (9)$$

where $L_{tail}[N] \equiv$ length of the tail in the particular contact sequence $[N]$ and $\langle L_{tail}\rangle \equiv$ ensemble average of $L_{tail}[N]$ for chains of length N. It is now a perfectly straightforward matter to calculate the percentages of the chain involved in loop, train, and tail formation, and these quantities we report below. Clearly, averages over all complexions $[N]$ of the sequence are required, and hence all complexions of $Z^{[i]}(0i|N)$ need to be calculated corresponding to all possible configurations of the sequence $[i]$ for $1 < i \leq N$. For this reason, the iterative convolution approach becomes prohibitively time consuming for the chain lengths of interest here. However, for short sequences ($N < 5$), the IC estimates were feasible and appeared to differ little from their noniterative counterparts.

Results and Discussion

We now consider the detailed resolution of the sequence into loop, train, and tail components as a function of chain length and solvent composition on the basis of the convolution approximation. Throughout we adopt a contact zone thickness of $\zeta = 0.0625$. Clearly, the choice of ζ governs the partitioning of the configurations, particularly the distribution between loops and chains. Higuchi et al.[8] have investigated the effect of various choices of ζ upon the resolution of loops, trains, and tails on the basis of MC simulations. These authors conclude that for thickly adsorbed layers at the boundary, the concept of a contact zone loses significance: this situation is likely to arise for long chains with significant chain-plane attraction. In the present case, this situation does not arise, and $\zeta = 0.0625$ represents a stringent and meaningful criterion for contact. First, however, we consider the underlying processes which determine the partitioning of the sequence into the three component classifications. We note from the outset that the development of loops and trains is sensitively dependent upon the segment density distribution $\rho(z|N)_{\eta\sigma_s}$ within the contact zone $z < 0.0625$, since this clearly determines returns to the boundary. In particular we see from Figure 1 that $\rho(0|N)_{\eta\sigma_s}$, the boundary contact value, systematically increases with packing fraction η, to an extent inversely related to solvent diameter. We anticipate that this behavior will reflect the dependence of loop, train, and tail states upon solvent composition.

In the absence of a solvent, the spatial probability distribution $Z(0i|N)$ of the ith segment along the normal to the boundary for a terminally attached sequence of N unit

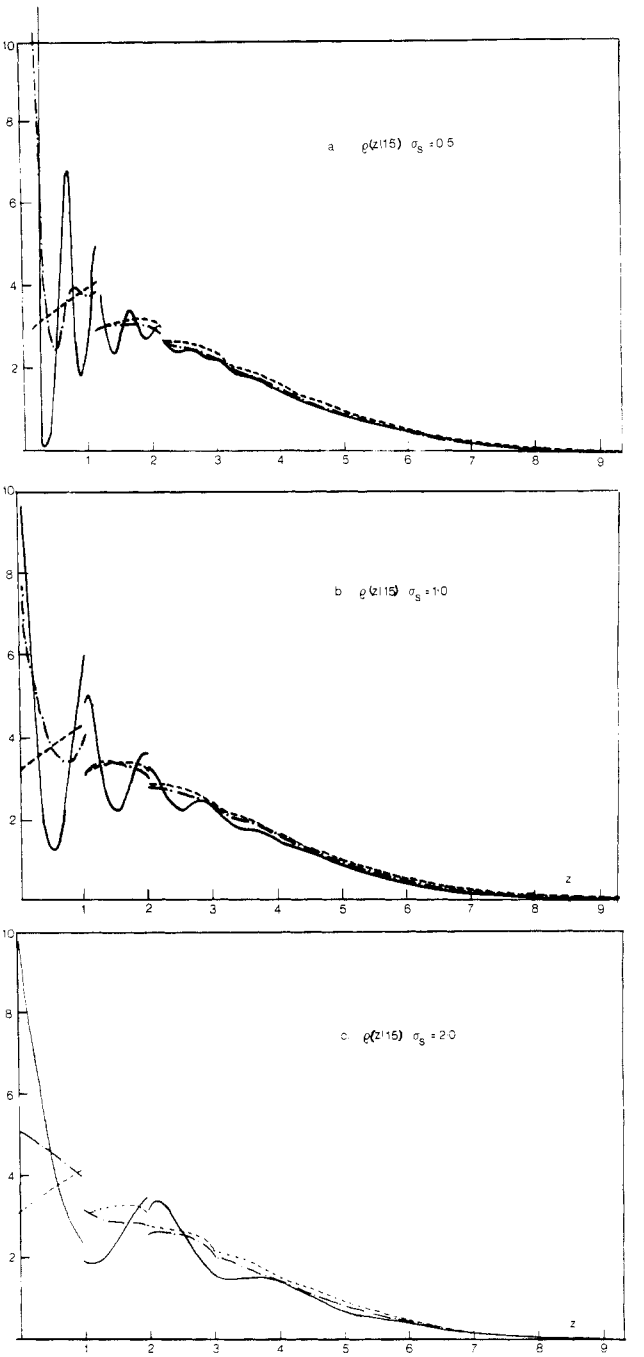

Figure 1. Development of $\rho(z|15)_{\eta\sigma_s}$ with packing fraction η and solvent diameter σ_s. (---) $\eta = 0$; (-·-) $\eta = 0.2$; (—) $\eta = 0.4$.

spheres is primarily determined by two competing processes. Sequential connectivity confines the ith segment to within a region $z \leq i-1$ along the normal to the accessible boundary, whilst configurational attrition due to the presence of the boundary introduces an effective "entropic repulsion" which acts to delocalize the sequence, although excluded volume effects will modify this simplified description.

Lattice-based analyses of isolated self-avoiding sequences confirm that C_N, the total number of distinct configurations of the N-mer, develops dramatically with increasing N.[5] It follows that with the introduction of a boundary the *attrition* of configurations, a_N, develops equally dramatically with increasing chain length: $\ln a_N$ is then a measure of the average entropic repulsion experienced by the sequence in the presence of a rigid boundary. Accordingly, we anticipate that the fraction of chain expelled from the vicinity of the boundary in the

form of tails will *increase* with increasing N. Indeed, the increasing entropic repulsion per particle associated with geometric attrition of the chain makes returns to the boundary in the form of loops and/or trains increasingly unlikely—the chain tending to be entirely in the form of tail states. Precisely this form of behavior has been previously reported, both on the basis of the convolution analysis and Monte Carlo simulation.[3]

However, as we explained earlier, relative to the disconnected particles which constitute the solvent, sequential connection to form a chain implies a configurational attrition per segment which also develops dramatically with chain length. Accordingly, with the introduction of a solvent, the increase in free energy per unit area associated with the presence of a boundary is minimized by the migration of chain segments rather than solvent particles to the interfacial region. This global minimization of configurational attrition results in a subtle balance of the entropic drives experienced by the sequence, the net effect of which is determined by the relative rates of attrition with increasing N for the two entropic processes.

With increasing sequence length, the rates of increase of attrition due to the two processes will reach a limiting ratio which ultimately governs the fraction of returns to the plane and hence the percentage of the chain in each of the three component states: loop, train, or tail.

It is instructive to compare the development of loops, trains, and tails in the presence of a solvent with the previously reported[2] zero-solvent case since in the latter situation attritional processes arise which may be specifically associated with the boundary, and whilst they persist with the introduction of solvent, they enable us to distinguish between those processes attributable to the boundary and those to be associated with the solvent. Accordingly we shall make the comparison throughout the subsequent discussion.

Tails

In the absence of a solvent, tail states account for >95% of chain configurations for self-avoiding sequences terminally attached to a rigid boundary with no chain-plane attraction (Figure 2). This result was determined on the basis of the convolution approximation[2] and subsequently confirmed by Monte Carlo simulation.[3] Moreover, with increasing chain length the increasing attrition per segment due to the introduction of a boundary ensured a corresponding increase in the percentage of the chain in tail configurations. With the introduction of a solvent, this behavior is dramatically modified: $\rho(z|N)_{\eta\sigma_s}$ within the contact zone $z < 0.0625$ develops rapidly with packing fraction (Figure 1) which can only result in the depletion in tail states. As discussed above, configurational attrition associated with the replacement of solvent particles by chain segments establishes a competing attritional drive *toward* the boundary, resulting in a systematic *decrease* of the tail percentage with increasing chain length. Whilst it appears that an asymptotic percentage of the sequence takes the form of tails with increasing N, the fraction is substantially reduced, with increased solvent packing fraction being ~83% at $\eta = 0.2$ and ~68% at $\eta = 0.4$, depending upon solvent diameter. Of course, there are corresponding redistributions amongst the loop and train states as we shall discuss below. The relative development of the two attritional processes with increasing chain length determines the gradient of the curves, whilst the asymptotic approach to a fixed percentage of the sequence in the form of tails suggests that the growth of the two attritional processes reaches a limiting ratio with increasing chain length, the ratio determining the asymptotic value. It is

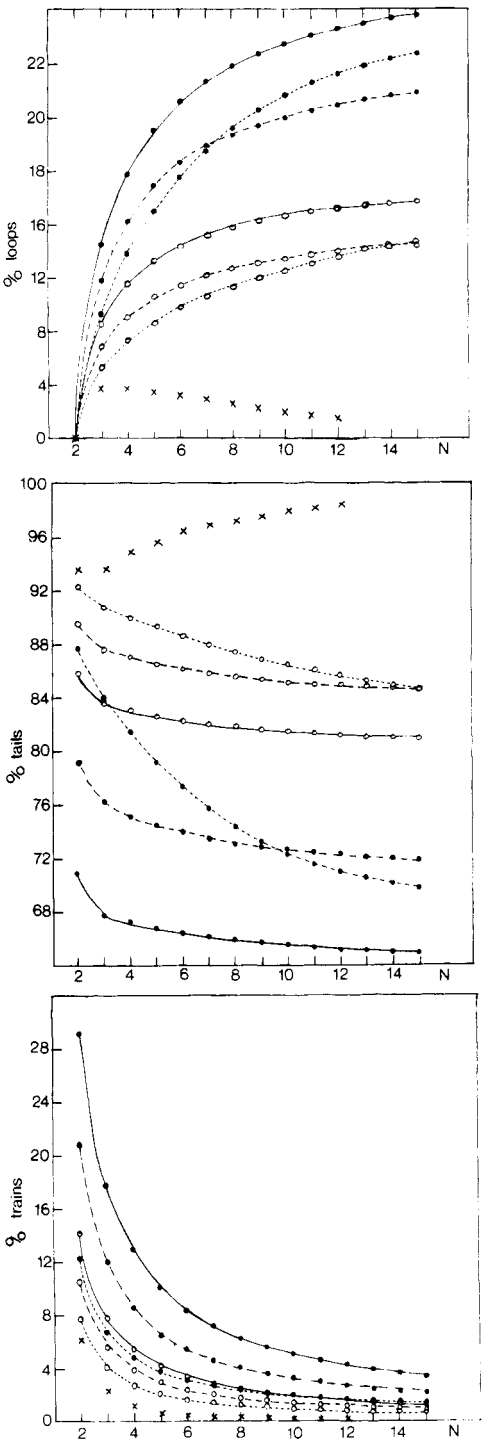

Figure 2. Percentage of chain in the form of (a) loops, (b) tails, and (c) trains as a function of chain length and solvent composition: (×) no solvent, (○) $\eta = 0.2$, (●) $\eta = 0.4$; (—) $\sigma_s = 0.5$, (– –) $\sigma_s = 1.0$, (- - - -) $\sigma_s = 2.0$.

clear that solvent diameter is instrumental in determining the attritional losses associated with the replacement of solvent by segment particles since the gradient of the curves for $\sigma_s = 2.0$ are substantially greater, at given packing fraction, than their smaller diameter solvent counterparts (Figure 2). Indeed, the $\sigma_s = 2.0$ curves actually cross the smaller solvent curves, a feature which is reflected in the development of the loop components.

As we might expect with the entropic drive toward the boundary associated with the introduction of the solvent, the average length of the sequence in the form of tails decreases with increasing packing fraction (Figure 3), showing a virtually linear dependence upon chain length.

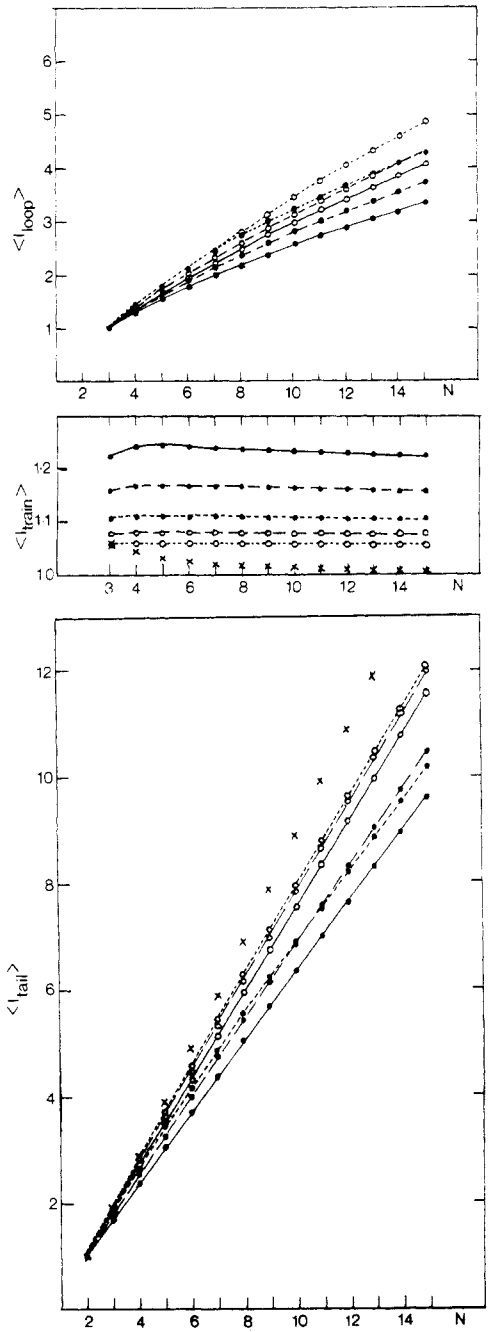

Figure 3. Average lengths of chain in the form of (a) loops, (b) trains, and (c) tails as a function of chain length and solvent composition: (×) no solvent, (○) $\eta = 0.2$, (●) $\eta = 0.4$; (—) $\sigma_s = 0.5$, (– –) $\sigma_s = 1.0$, (- - - -) $\sigma_s = 2.0$.

In fact, a least-squares quadratic fit to the convolution data on the basis of the asymptotic relation

$$\langle l_{tail} \rangle \sim (N-1)^x L t N \rightarrow \infty$$

yields the limiting exponents x listed in Table I. The exponents appear to show a relatively weak dependence upon solvent composition and are consistently below both the convolution and MC estimates determined in the absence of a solvent. For comparison, the much earlier result of Roe[4] is shown which takes only partial account of excluded volume effects and relates to the case of weak chain-plane attraction. Nevertheless, the results are in good overall agreement, with the solvent effecting a marginal decrease of the exponent below linearity.

Finally (Figure 4), we show the average number of tails per chain which, except for the shortest sequences, appears insensitive to solvent composition with an asymptotic

Table I
Limiting Exponents as $N \rightarrow \infty$ of the Loop, Train, and Tail Length Dependences upon Chain Length

σ_s	$\eta = 0.2$	$\eta = 0.4$	MC, $\eta = 0.0$	Roe, $\eta = 0.0$
		Loops		
0.5	0.60	0.51	0.57	0.50
1.0	0.62	0.54		
2.0	0.69	0.44		
		Trains		
0.5	0.00	0.00	0.00	0.00
1.0	0.00	0.00		
2.0	0.00	0.00		
		Tails		
0.5	0.98	0.97	1.00	1.00
1.0	0.98	0.97		
2.0	0.93	0.92		

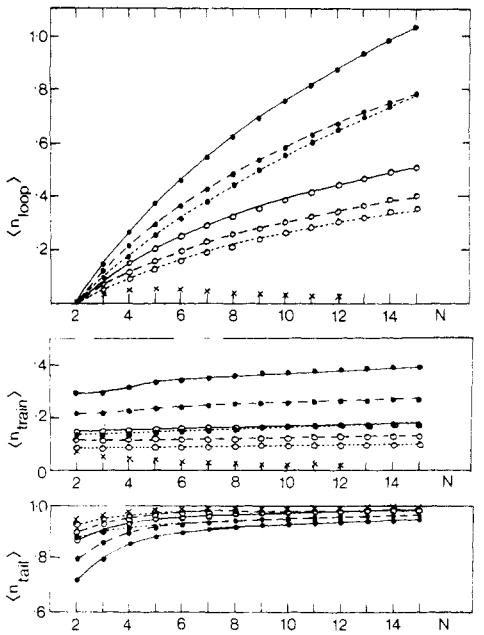

Figure 4. Average number of (a) loops, (b) trains, and (c) tails in a chain as a function of length and solvent composition: (×) no solvent, (○) $\eta = 0.2$, (●) $\eta = 0.4$; (—) $\sigma_s = 0.5$, (– –) $\sigma_s = 1.0$, (- - - -) $\sigma_s = 2.0$.

tendency toward every chain terminating in a tail configuration. Even so, it is quite clear that this tendency is most pronounced for large solvent particles at low packing fraction for which $\rho(z|N)_{\eta\sigma_s}$ at $z < 0.0625$ is relatively small: this conclusion is confirmed by the zero solvent result.

Loops

Configurational attrition due to the presence of a boundary accounted for the minimal contribution of loops (<4%) to chain configurations in the absence of a solvent (Figure 2)[2,3]—a component which decreased, moreover, with increasing chain length. The introduction of a solvent again substantially modifies the development of loops which now account for ~30% of the chain configurations at a packing fraction of $\eta = 0.4$ (Figure 2). The loop component increases steadily with increasing chain length, asymptotically approaching a limiting fraction of the chain configurations, and largely complementing the asymptotic development of the tail states. Again, a fairly subtle dependence upon solvent composition is apparent but is understood in terms of the processes discussed above for tails.

The average length of loops appears to grow slowly with chain length, although there does appear to be a consistent reduction in $\langle l_{loop} \rangle$ with decreasing solvent diameter and

increasing packing fraction (Figure 3): at given chain length the loop size decreases by <15% with the introduction of a solvent over the range of chain lengths investigated, whilst the number of loops increases dramatically (Figure 4). We have noted previously[3] on the basis of Monte Carlo investigations in the absence of a solvent that there appears to be a bimodal distribution of loop sizes—chains tend to loop in either large or small denominations. This we understood in terms of the greater attritional losses within the sequence associated with a midchain return to the boundary to form loops, rather than near the ends, thereby accounting for the bimodal distribution of loop sizes. Asymptotic relations of the form

$$\langle l_{\text{loops}} \rangle \sim (N-1)^x LtN \rightarrow \infty$$

yield the exponents listed in Table I. At low packing fractions, the exponent appears to increase with solvent diameter, whilst at $\eta = 0.4$, apart from showing a substantially weaker dependence upon chain length, it also seems to maximize at $\sigma_s = 1.0$. Whether this dependence upon solvent diameter is a real feature of the system due, perhaps, to geometrical constraints upon loop size at the boundary given the size of the solvent particle, or an artifact of the approximation is not clear at this stage, and further consideration here is not worthwhile. However, we do believe that the exponent dependence upon solvent packing fraction is real, and the stronger dependence of loop size upon chain length at $\eta = 0.2$ than at either $\eta = 0$ or 0.4 is attributed to the effective self-cancellation of the two attritional processes, one of which dominates at $\eta = 0$ and the other at $\eta = 0.4$. The overall consistency with the results obtained in the absence of a solvent is good, moreover, as is the comparison with Roe's estimate[4] in which excluded volume effects are only partially included.

While the size of loops decreases only slightly with packing fraction (Figure 3), the *number* of loops almost doubles as $\eta = 0.2 \rightarrow 0.4$ (Figure 4) and at $\eta = 0.4$ is almost 50 times greater than in the absence of a solvent for the longest sequences investigated. At any given chain length, the additional entropic drive associated with the presence of the solvent evidently predisposes an increase in returns to the boundary in the form of loops of smaller denominations: hence the increase in number and decrease in loop size with increasing packing fraction.

Trains

Regardless of the presence of solvent, trains, in the form of at least one-link returns, represent a minimal and decreasing component of chain configurations with increasing chain length. Increasing solvent packing fraction does appear to increase the asymptotic fraction of the sequence in the form of trains (Figure 2), which is readily understood in terms of the attritional processes described above and, more immediately, in terms of the solvent dependence of the segment density distribution $\rho(z|N)_{\eta\sigma_s}$ within the contact zone $z < 0.0625$. In fact, the number of trains doubles as $\eta = 0.2 \rightarrow 0.4$ and is increased by a factor $\sim$ 100 over the zero solvent case, while the average length of trains increases by up to 23% on the zero solvent value for $\eta = 0.4$ and $\sigma_s = 0.5$ for the range of chain lengths investigated here. Asymptotic representations of $\langle L_{\text{train}} \rangle$ upon chain length yield the exponents listed in Table I, and in every case a least-squares quadratic fit to the convolution data confirms the independence of $\langle L_{\text{train}} \rangle$ upon chain length for given solvent composition, at least for the range of chain lengths investigated here. Even though trains at $\eta = 0.4$ are almost 100 times more likely than in the absence of solvent, they still constitute only a very small component of chain configurations at the boundary, basically in the form of one-link returns, and any development of $\langle L_{\text{train}} \rangle$ with N is unlikely to be apparent for the range of chain lengths investigated here.

As previously observed,[1] while the segment density distribution normal to the boundary is sensitively dependent upon solvent composition, the mean thickness $\langle z_N \rangle$ of the adsorbed layer is not. We therefore conclude that the constitution of the layer in terms of loops, trains, and tails may be effectively controlled by means of solvent composition.

Acknowledgment. I thank Ruby Turner for performing the numerical computations and ARGS for financial support. I also thank the referees for some helpful suggestions.

References and Notes

(1) Croxton, C. A. *Macromolecules* **1987**, *20*, 2847.
(2) Croxton, C. A. *J. Phys. A: Math. Gen.* **1986**, *19*, 2353.
(3) Croxton, C. A. *J. Phys. A: Math. Gen.* **1986**, *19*, 987.
(4) Roe, R.-J. *J. Chem. Phys.* **1965**, *43*, 1591; **1965**, *44*, 4264. Simha, R.; Frisch, H. L.; Eirich, R. F. *J. Phys. Chem.* **1953**, *57*, 584. Silberberg, A. *J. Phys. Chem.* **1962**, *66*, 1872, 1884; *J. Chem. Phys.* **1967**, *46*, 1105. Chen, D.; Mitchell, D. J.; Ninham, B. W.; White, L. *J. Chem. Soc., Faraday Trans. 2* **1975**, *71*, 235.
(5) Torrie, G. M.; Middlemiss, K.; Bly, S. H. P.; Whittington, S. G. *J. Chem. Phys.* **1976**, *65*, 1867.
(6) Clark, A. T.; Lal, M. *J. Chem. Soc., Faraday Trans. 2*, **1978**, *74*, 1857; **1981**, *77*, 981.
(7) Croxton, C. A. In *Fluid Interfacial Phenomena*; Croxton, C. A., Ed.; Wiley: Chichester and New York, 1986.
(8) Higuchi, A.; Rigby, D.; Stepto, F. I. In *Adsorption from Solution*; Ottewill, R. H., Rochester, C. H., Smith, A. L., Eds.; Academic: New York, 1983; p 273 et seq.
(9) Dickman, R.; Croxton, C. A. submitted for publication in *J. Chem. Phys.*